# UNIVERSITY *of York*

This is a repository copy of *Magnetic Shielding, Aromaticity, Antiaromaticity and Bonding in the Low-Lying Electronic States of Benzene and Cyclobutadiene*.

White Rose Research Online URL for this paper:
https://eprints.whiterose.ac.uk/106786/

Version: Accepted Version

## Article:

White Rose
university consortium
Universities of Leeds, Sheffield & York

eprints@whiterose.ac.uk
https://eprints.whiterose.ac.uk/

# Magnetic Shielding, Aromaticity, Antiaromaticity and Bonding in the Low-Lying Electronic States of Benzene and Cyclobutadiene

Peter B. Karadakov*, Peter Hearnshaw and Kate E. Horner

Department of Chemistry, University of York, Heslington, York YO10 5DD, UK
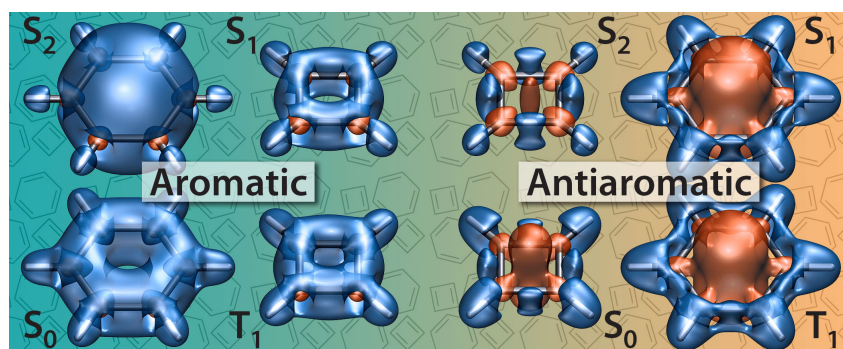
**ABSTRACT:** Aromaticity, antiaromaticity and their effects on chemical bonding in the ground states ($S_0$), lowest triplet states ($T_1$), and the first and second singlet excited states ($S_1$ and $S_2$) of benzene ($C_6H_6$) and square cyclobutadiene ($C_4H_4$) are investigated by analysing the variations in isotropic magnetic shielding around these molecules in each electronic state. All shieldings are calculated using state-optimized $\pi$-space complete-active-space self-consistent field (CASSCF) wavefunctions constructed from gauge-including atomic orbitals (GIAOs), in the 6-311++G(2d,2p) basis. It is shown that the profoundly different shielding distributions in the $S_0$ states of $C_6H_6$ and $C_4H_4$ represent aromaticity and antiaromaticity "fingerprints" which are reproduced in other electronic states of the two molecules and allow classification of these states as aromatic ($S_0$ and $S_2$ for $C_6H_6$, $T_1$ and $S_1$ for $C_4H_4$) or antiaromatic ($S_0$ and $S_2$ for $C_4H_4$, $T_1$ and $S_1$ for $C_6H_6$). $S_2$ $C_6H_6$ is predicted to be even more aromatic than $S_0$ $C_6H_6$. As isotropic shielding isosurfaces and contour plots show very clearly the effects of aromaticity and antiaromaticity on chemical bonding, these can be viewed, arguably, the most succinct visual definitions of the two phenomena currently available.

# 1 INTRODUCTION

Whereas, up until recently, excited state aromaticity and antiaromaticity were regarded mainly as theoretical hypotheses (for an overview of the area, see the comprehensive review by Kilså, Ottosson *et al.*[1]), now there are convincing experimental proofs, furnished by Kim, Osuka and co-workers, of aromaticity reversals in the lowest triplet states of bis-rhodium hexaphyrins,[2] and in the lowest singlet states of 1,3-phenylene-strapped [26]- and [28]hexaphyrins.[3] The first of these targets the better-known excited state aromaticity associated with Baird's rule,[4] according to which the familiar $4n + 2$ and $4n$ rules for ground-state aromaticity in cyclic conjugated hydrocarbons are switched over in their lowest triplet states: rings with $4n$ $\pi$ electrons come out as aromatic while those with $4n + 2$ $\pi$ electrons end up as antiaromatic; the second one addresses an analogous effect expected in the respective lowest singlet excited states.[5,6] The increased interest in excited state aromaticity and antiaromaticity[1,7] is creating demand for theoretical tools that are capable of providing detailed accounts of these phenomena and their implications for the properties of the excited states; such tools can aid the design of organic compounds with potential applications in organic electronics and photovoltaics.[1] In this paper we show that these purposes are served very well by analyses of the off-nucleus isotropic magnetic shielding isosurfaces and contour plots for excited states.

The behavior of magnetic shielding tensors, $\boldsymbol{\sigma}(\mathbf{r})$, calculated at various positions $\mathbf{r}$ within the space surrounding a molecule carries a wealth of information about chemical bonding and, for cyclic conjugated systems, about aromaticity. Off-nucleus isotropic magnetic shieldings, $\sigma_{\mathrm{iso}}(\mathbf{r}) = \frac{1}{3}[\sigma_{xx}(\mathbf{r}) + \sigma_{yy}(\mathbf{r}) + \sigma_{zz}(\mathbf{r})]$, and out-of-plane components of $\boldsymbol{\sigma}(\mathbf{r})$, $\sigma_{zz}(\mathbf{r})$, are involved in the definitions of nucleus-independent chemical shifts (NICS), popular single-point aromaticity indices introduced by Schleyer and co-workers. The original NICS index, NICS(0),[8] was defined as $-\sigma_{\mathrm{iso}}$(at ring center); subsequent attempts to improve the accuracy of relative aromaticity predictions led to the formulation of further NICS indices including NICS(1) = $-\sigma_{\mathrm{iso}}$(at 1 Å above ring center),[9,10] NICS(0)$_{zz}$ = $-\sigma_{zz}$(at ring center),[11,12] NICS(1)$_{zz}$ = $-\sigma_{zz}$(at 1 Å above ring center),[13] as well as various "dissected" NICS indices (for details, see *e.g.* Ref. 13).

An essential feature of NICS(0), NICS(1), NICS(0)$_{zz}$ and NICS(1)$_{zz}$ is that these indices can be calculated not just using the Hartree-Fock (HF) method and density functional theory (DFT), but also by means of post-HF methods accounting for electron correlation effects such as MP2 (second order Møller-Plesset perturbation theory) and CASSCF (complete-active-space self-consistent field). NICS(0), NICS(1), NICS(0)$_{zz}$ and NICS(1)$_{zz}$ values obtained using CASSCF wavefunctions constructed from gauge-including atomic orbitals (GIAOs) were amongst the magnetic criteria used in the first post-HF ab initio assessments of the aromaticities of the low-lying electronic states of benzene, cyclobutadiene and cyclooctatetraene.[5,6] According to the results reported in Refs. 5,6, these molecules

which, in their electronic ground states ($S_0$), are regarded as classical examples of aromatic and antiaromatic systems, exhibit complete changeovers of aromatic character in their lowest triplet states ($T_1$) and first singlet excited states ($S_1$): Benzene ($D_{6h}$ symmetry) switches from aromatic in $S_0$ to antiaromatic in $T_1$ and $S_1$, whereas cyclobutadiene and cyclooctatetraene in their highest-symmetry geometries ($D_{4h}$ and $D_{8h}$, respectively), switch from antiaromatic in $S_0$ to aromatic in $T_1$ and $S_1$. The aromaticity reversals between different electronic states of benzene, cyclobutadiene and cyclooctatetraene have been confirmed by Feixas, Solà *et al.*[14] through an alternative approach that does not utilize magnetic properties, but involves the examination of electronic delocalization indices calculated using CASSCF wavefunctions.

A more versatile approach which goes beyond the single-point NICS idea is to examine how isotropic shielding varies within the space surrounding the molecular framework.[15–22] Detailed $\sigma_{\mathrm{iso}}(\mathbf{r})$ isosurfaces and contour plots constructed from dense regular grids of $\sigma_{\mathrm{iso}}(\mathbf{r})$ values (as established in Refs. 19–22, a reasonable compromise between level of detail and computational effort is achieved by using a spacing of 0.05 Å) allow very clear distinction between aromaticity and antiaromaticity in the electronic ground states of benzene and cyclobutadiene and reveal how pronounced differences in aromatic character are reflected in chemical bonding.[19] These isosurfaces and contour plots also help differentiate between the aromaticities of heterocycles with one and two heteroatoms,[20,21] and provide an easy-to-interpret picture of chemical bonding in hydrocarbons, which is more detailed than the traditional description in terms of the total electronic density.[22] The analysis of the off-nucleus magnetic isotropic shielding as a function of position addresses some of the more important criticisms towards various types of single-point NICS, including the certain degree of arbitrariness in the choice of the positions at which single-point NICS are calculated, and the fact that a single number might not be able to carry the information content required to characterize the aromaticity of a system—for example, it is has been shown that different ring current maps can produce nearly indistinguishable single-point NICS values.[23,24]

In this paper we use off-nucleus isotropic magnetic shielding isosurfaces and contour plots to study aromaticity, antiaromaticity and chemical bonding in the low-lying electronic states of benzene and square cyclobutadiene. The electronic states examined, for both molecules, are $S_0$, $T_1$, $S_1$ and $S_2$, a selection similar to that from Ref. 5, with the addition of the second singlet excited state ($S_2$) of benzene. Following past experience with evaluating magnetic properties of benzene and cyclobutadiene,[5,19] in order to treat the different electronic states of the two molecules at a level of theory producing comparable qualitatively correct results, all calculations are carried out using state-optimized $\pi$-space CASSCF-GIAO wavefunctions. Previous research[19] revealed profound differences between the isotropic shielding distributions in the ground electronic states of benzene and square cyclobutadiene: All carbon-carbon bonds in benzene were found to be enclosed within a doughnut-shaped region of increased shielding, in-

dicative of strong bonding interactions, whereas square cyclobutadiene was shown to have a strongly deshielded dumbbell-shaped region in the center of the molecule, causing partial disruption of the carbon-carbon bonds and antiaromatic destabilization. Our main aim is to establish whether similar differences are also observed in the low-lying electronic excited states of these molecules which would provide strong support, from an approach free from the shortcomings of single-point NICS indices, for the conclusions about aromaticity and antiaromaticity in the $T_1$ and $S_1$ states made in Ref. 5, help decide on the aromaticities of the $S_2$ states, and prove that analyses of the off-nucleus isotropic magnetic shielding isosurfaces and contour plots can be used to obtain detailed information about aromaticity, antiaromaticity and bonding in the excited states of key organic compounds.

## 2 COMPUTATIONAL PROCEDURE

All CASSCF-GIAO calculations on benzene and cyclobutadiene reported in this paper were carried out using the MCSCF-GIAO (multiconfigurational SCF with GIAOs) methodology introduced in Refs. 25, 26 and implemented in the Dalton 2016.0 program package,[27] within the 6-311++G(2d,2p) basis.

The $S_0$ ($1\,^1A_{1g}$), $T_1$ ($1\,^3B_{1u}$), $S_1$ ($1\,^1B_{2u}$) and $S_2$ ($1\,^1B_{1u}$) electronic states of benzene were described using state-optimized $\pi$-space CASSCF(6,6) wavefunctions (with '6 electrons in 6 orbitals'), at the experimental $D_{6h}$ gas-phase ground-state geometry with C–C and C–H bond lengths of 1.3964 Å and 1.0831 Å, respectively, established through analysis of the $\nu_4$ vibration-rotation bands of $C_6H_6$ and $C_6D_6$.[28]

The calculations on the $S_0$ ($1\,^1B_{1g}$), $T_1$ ($1\,^3A_{2g}$), $S_1$ ($1\,^1A_{1g}$) and $S_2$ ($1\,^1B_{2g}$) electronic states of square cyclobutadiene employed state-optimized $\pi$-space CASSCF(4,4) wavefunctions (with '4 electrons in 4 orbitals'), at the $D_{4h}$ geometry with C–C and C–H bond lengths of 1.447 Å and 1.076 Å, respectively, optimized through a multireference averaged quadratic coupled cluster (MR-AQCC) approach with orbitals taken from state-averaged $\pi$-space CASSCF(4,4) wavefunctions including the ground state, lowest triplet state and two lowest singlet excited states (SA-4-CASSCF), within the cc-pVTZ basis.[29]

The geometries of benzene and square cyclobutadiene chosen for the current calculations are identical to those used in Refs. 5, 19.

As a result of the decision to use ground-state geometries for all excited states, the comparisons between the properties of the electronic states of benzene and cyclobutadiene are in the context of vertical excitations. While the lowest energy geometries of aromatic electronic states can be expected to remain reasonably similar to the $D_{6h}$ and $D_{4h}$ geometries of benzene and cyclobutadiene, respectively, used in the calculations, the lowest-energy geometries of electronic states classified as antiaromatic are likely to exhibit significantly lower symmetries, due to distortions that reduce the antiaromatic character, such as

the well-known $D_{4h}$ to $D_{2h}$ ("square" to "rectangle") symmetry reduction in the electronic ground state of cyclobutadiene.

Following previous work on NICS[5,6,30] and ring currents[31] in triplet systems, the CASSCF-GIAO isotropic shieldings in the $T_1$ states of benzene and cyclobutadiene reported in this paper include the contributions arising from the perturbation to the wavefunction only (often referred to as "orbital" contributions in single-determinant approaches). While this choice is convenient for the purposes of the current study, as the values reported for a triplet state become directly comparable to those for singlet states, a more rigorous treatment would need to take into account the large terms associated with the interaction between the electronic spin angular momentum and the magnetic field.[32,33]

The grids of points used in the construction of $\sigma_{\mathrm{iso}}(\mathbf{r})$ isosurfaces and contour plots for the $S_0$, $T_1$, $S_1$ and $S_2$ electronic states of benzene and cyclobutadiene were defined similarly to the grids employed for the $S_0$ electronic states of these molecules in Ref. 19: The grid for each molecule is regular, with a spacing of 0.05 Å, includes $141^3$ points ($C_6H_6$) or $101^3$ points ($C_4H_4$), and takes the shape of a cube with edges of 7 Å ($C_6H_6$) or 5 Å ($C_4H_4$), centered at the origin of a center-of-mass right-handed Cartesian coordinate system in which the $z$ axis is perpendicular to the molecular plane and the $x$ axis passes through the midpoints of two carbon-carbon bonds. In order to reduce computational effort, for each electronic state $\sigma_{\mathrm{iso}}(\mathbf{r})$ values were calculated only at the $71^3$ points ($C_6H_6$) or $51^3$ points ($C_4H_4$) within one octant of the respective grid and replicated by symmetry. For visualization purposes, all $\sigma_{\mathrm{iso}}(\mathbf{r})$ values obtained for the various electronic states of $C_6H_6$ and $C_4H_4$ were assembled in GAUSSIAN cube files.[34]

# 3    RESULTS AND DISCUSSION

The energies of the CASSCF(6,6)/6-311++G(2d,2p) wavefunctions for the $S_0$, $T_1$ and $S_1$ states of benzene and the CASSCF(4,4)/6-311++G(2d,2p) wavefunctions for the $S_0$, $T_1$, $S_1$ and $S_2$ states of square cyclobutadiene computed in this paper turned out to be exactly the same as those reported in Ref. 5. As it was noted in Ref. 5, the CASSCF(6,6)/6-311++G(2d,2p) $S_0$ to $T_1$ and $S_0$ to $S_1$ vertical excitation energies for benzene agree very well with experimental data[35,36] and higher-level theoretical estimates;[37] in square cyclobutadiene, the CASSCF(4,4)/6-311++G(2d,2p) $S_0$ to $T_1$, $S_0$ to $S_1$ and $S_0$ to $S_2$ vertical excitation energies show some improvement over CASSCF(4,4)/6-31G results[38] but, due to the limited sizes of the singlet and triplet '4 in 4' active spaces, remain somewhat higher than the values obtained using more advanced theoretical methods.[29]

The CASSCF(6,6)/6-311++G(2d,2p) calculation for the $S_2$ electronic state of benzene produced an energy of $-230.550\ 895$ au which corresponds to an $S_0$ to $S_2$ vertical excitation energy of 7.82 eV. This vertical excitation energy is higher than the experimental value of 6.20 eV,[36] but in line with other

Table 1: Carbon and proton isotropic shieldings, and NICS(0), NICS(1), NICS(0)$_{zz}$ and NICS(1)$_{zz}$ values for the $S_0$, $T_1$, $S_1$ and $S_2$ electronic states of benzene and square cyclobutadiene (in ppm). For further details, see text.

| Molecule | State | $\sigma_{\text{iso}}(^{13}C)$ | $\sigma_{\text{iso}}(^{1}H)$ | NICS(0) | NICS(1) | NICS(0)$_{zz}$ | NICS(1)$_{zz}$ |
|---|---|---|---|---|---|---|---|
| $C_6H_6$ | $S_0$ ($1\,^1A_{1g}$) | 73.52 | 24.90 | –8.17 | –9.53 | –12.21 | –27.83 |
| | $T_1$ ($1\,^3B_{1u}$) | 81.89 | 29.31 | 39.63 | 30.10 | 130.54 | 90.61 |
| | $S_1$ ($1\,^1B_{2u}$) | 78.69 | 29.54 | 45.81 | 34.67 | 145.90 | 102.76 |
| | $S_2$ ($1\,^1B_{1u}$) | 75.42 | 21.25 | –39.08 | –36.68 | –119.47 | –117.59 |
| | | | | | | | |
| $C_4H_4$ | $S_0$ ($1\,^1B_{1g}$) | 68.24 | 27.60 | 36.41 | 28.23 | 145.91 | 88.14 |
| | $T_1$ ($1\,^3A_{2g}$) | 71.75 | 25.15 | –3.74 | –6.54 | 24.26 | –16.47 |
| | $S_1$ ($1\,^1A_{1g}$) | 54.80 | 23.96 | 3.44 | –4.28 | 24.61 | –16.38 |
| | $S_2$ ($1\,^1B_{2g}$) | 15.85 | 22.88 | 22.10 | 12.86 | 77.09 | 31.24 |

theoretical results coming from $\pi$-space wavefunctions, for example, the result of a CASSCF(6,6) calculation in an ANO basis was almost the same, 7.85 eV,[39] and a much larger spin-coupled valence bond (SCVB) wavefunction yielded 7.49 eV.[37] In this case, achieving better agreement with experiment requires inclusion of dynamic correlation between the electrons in $\sigma$ and $\pi$ orbitals: Second-order perturbation theory with a CASSCF(6,12) $\pi$-space reference (CASPT2) gave an $S_0$ to $S_2$ vertical excitation energy of 6.10 eV.[39]

The carbon and proton isotropic shieldings, and the NICS(0), NICS(1), NICS(0)$_{zz}$ and NICS(1)$_{zz}$ values for the $S_0$, $T_1$, $S_1$ and $S_2$ electronic states of benzene and square cyclobutadiene, extracted from the current calculations of shielding tensors at the respective grids of points, are shown in Table 1. The numbers for states other than the $S_2$ electronic state of benzene are identical to those reported in Ref. 5 and have been included in order to facilitate comparison with the rather unexpected magnetic features of this state. The NICS(0), NICS(1), NICS(0)$_{zz}$ and NICS(1)$_{zz}$ values for the $S_2$ electronic state of benzene indicate that in this state benzene becomes highly aromatic, significantly more so than in its ground electronic state ($S_0$). This conclusion is reinforced by the observation that $S_2$ benzene exhibits significant proton deshielding—the corresponding $\sigma_{\text{iso}}(^{1}H)$ value is 3.65 ppm lower than its $S_0$ counterpart.

Interestingly, the findings of Feixas, Solà et al.[14] about the $S_2$ electronic state of benzene are rather different. According to these authors, the $S_2$ and $S_3$ electronic states of benzene are degenerate; some electronic delocalization indices show that these states exhibit lower aromaticity than $S_0$, whereas other

electronic delocalization indices suggest that $S_2$ and $S_3$ are either more antiaromatic or less antiaromatic than $S_1$. In fact, the $S_2$ ($1\,^1B_{1u}$) electronic state of benzene is well-known to be non-denegerate (see *e.g.* Refs. 37, 39). The reported degeneracy of $S_2$ and $S_3$ and identical $S_0$ to $S_2$ and $S_0$ to $S_3$ vertical excitation energies of 8.17 eV indicate that the authors of Ref. 14 were not looking at $S_2$ and $S_3$, but at the two components of the degenerate $S_4$ ($1\,^1E_{2g}$). The order of the benzene $S_3$ ($1\,^1E_{1u}$) and $S_4$ ($1\,^1E_{2g}$) electronic states is reversed in $\pi$-space CASSCF(6,6) calculations; the corresponding vertical excitation energies obtained in an ANO basis are 9.29 eV ($S_0$ to $S_3$) and 8.11 eV ($S_0$ to $S_4$), respectively.[39] Getting the $S_3$ and $S_4$ states in the correct order requires inclusion of dynamic correlation between the electrons in $\sigma$ and $\pi$ orbitals, for example, through CASPT2.[39]

The $^{13}$C isotropic shieldings in benzene increase by 5.17 ppm on passing from $S_0$ to $S_1$, but then decrease by 3.27 ppm between $S_1$ and $S_2$. These differences are much smaller in magnitude than the substantial decreases of the $^{13}$C isotropic shieldings in the $S_0$, $S_1$, $S_2$ sequence of electronic states in square cyclobutadiene. Thus, while it can be expected that, in general, electronic excitation would be accompanied by nuclear deshielding, especially for heavier nuclei,[5] some low-lying electronic states may show exceptions.

The spatial variations in isotropic shielding, $\sigma_{iso}(\mathbf{r})$, for the $S_0$, $T_1$, $S_1$ and $S_2$ states of benzene and square cyclobutadiene are illustrated in Figures 1–6. The isotropic shielding isosurfaces and contour plots for the ground electronic states ($S_0$) of both molecules are very similar to the respective isosurfaces and contour plots obtained previously using CASSCF(6,6)-GIAO and CASSCF(4,4)-GIAO wavefunctions in the smaller 6-311++G(d,p) basis.[19] While the current $S_0$ isotropic shielding isosurfaces calculated in the 6-311++G(2d,2p) basis (see Figures 1 and 2) are visually indistinguishable from the corresponding 6-311++G(d,p) isosurfaces,[19] the more detailed $S_0$ $\sigma_{iso}(\mathbf{r})$ contour plots (see Figures 3–6) indicate that the use of a larger basis leads to some deshielding in regions close to the ring centers.

The shapes of the isotropic shielding isosurfaces and contour plots in Figures 1–6 show clearly that the profoundly different isotropic shielding distributions in the electronic ground states of benzene and square cyclobutadiene, reported initially in Ref. 19 and confirmed in the current work, can be viewed as aromaticity and antiaromaticity "fingerprints" which are closely reproduced in other low-lying electronic states of the two molecules and allow the unambiguous classification of these states as aromatic or antiaromatic.

In the $S_0$ electronic state of benzene the carbon ring is enclosed within a doughnut-shaped region of increased shielding, inside which $\sigma_{iso}(\mathbf{r})$ reaches 45.07 ppm at the midpoint of each carbon-carbon bond. Similar pictures, suggesting strong bonding interactions and aromatic stability (although not up to $S_0$ benzene levels), are observed in the $T_1$ and $S_1$ electronic states of square cyclobutadiene. In both of these states the positions of maximal shielding near carbon-carbon bonds, corresponding to $\sigma_{iso}(\mathbf{r})$

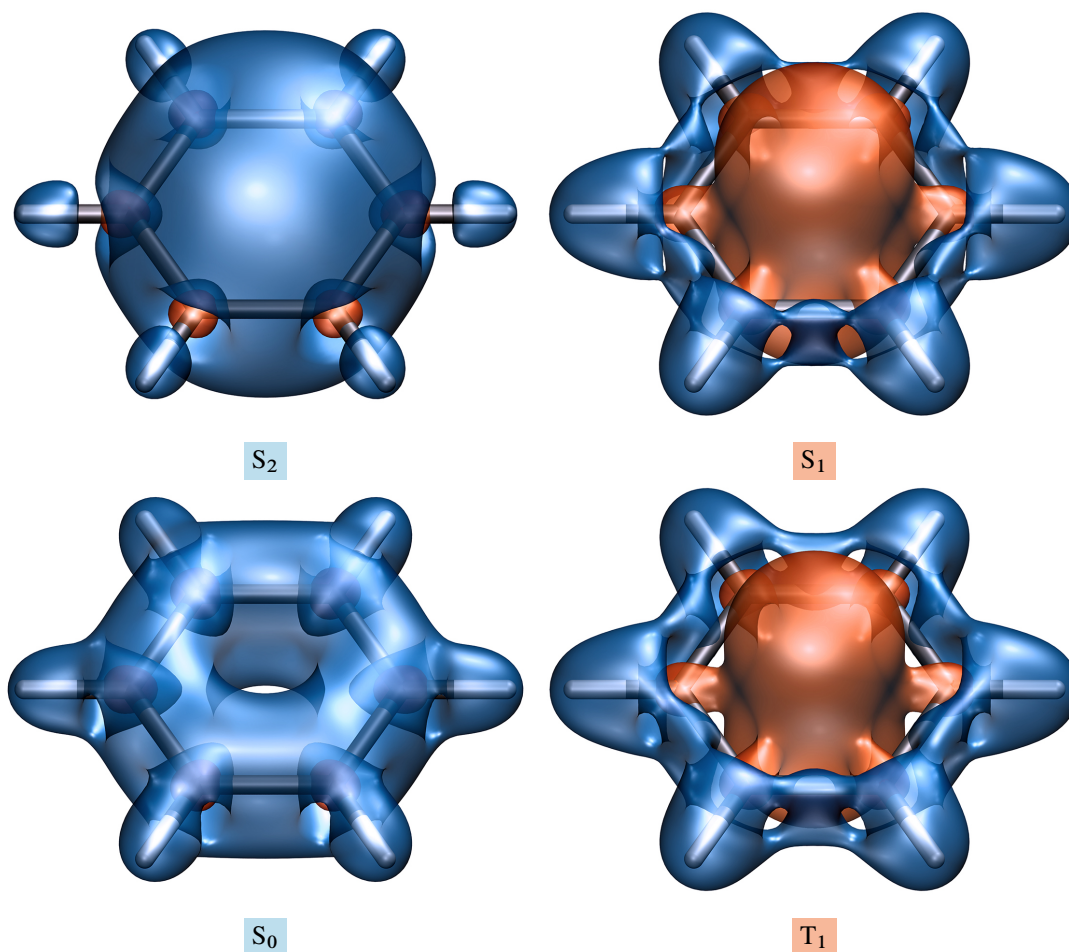Figure 1: Isotropic shielding isosurfaces at $\sigma_{\mathrm{iso}}(\mathbf{r}) = \pm 16$ ppm for the $S_0$, $T_1$, $S_1$ and $S_2$ states of benzene obtained using state-optimized $\pi$-space CASSCF(6,6)-GIAO/6-311++G(2d,2p) wavefunctions (positive isovalue in blue).

values of 39.14 ppm for $T_1$ and 35.34 ppm for $S_1$, are displaced towards the exterior of the ring (see Figure 4). In the $S_2$ electronic state of benzene the interior of the carbon ring is so intensely shielded that, in order to obtain a doughnut-shaped isotropic shielding isosurface, the $\sigma_{\mathrm{iso}}(\mathbf{r})$ isovalue would need to exceed 40 ppm (see Figure 5). In this state, the maximal shieldings near carbon-carbon bonds reach 59.74 ppm, at positions displaced towards the interior of the ring (see Figure 3).

Antiaromatic destabilization in the $S_0$ electronic state of square cyclobutadiene can be attributed to the presence of a markedly deshielded dumbbell-shaped region in the center of the molecule which disrupts the linkages between the shielded regions corresponding to individual carbon-carbon bonds, reduces shielding within these regions and displaces them to off-bond locations outside the ring. The maxima of 24.38 ppm achieved within shielded regions near carbon-carbon bonds are significantly lower than the corresponding values for aromatic electronic states. Similar central deshielded regions affecting adversely bonding along the respective carbon frameworks appear, even more prominently, in the $T_1$ and
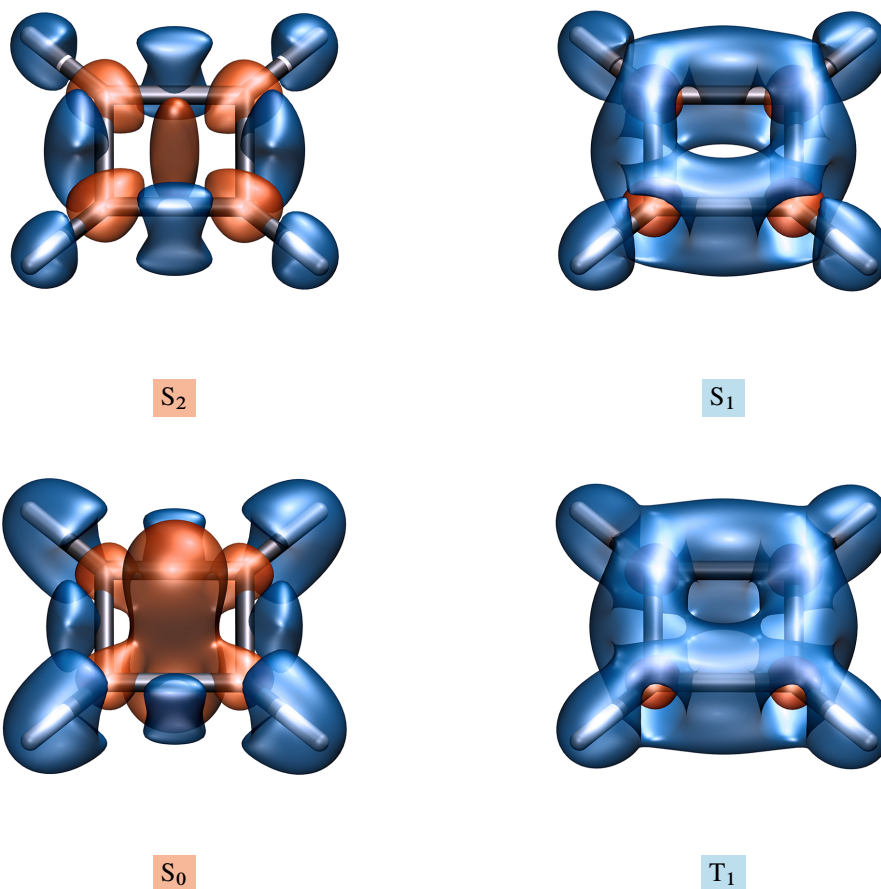
Figure 2: Isotropic shielding isosurfaces at $\sigma_{\text{iso}}(\mathbf{r}) = \pm 16$ ppm for the $S_0$, $T_1$, $S_1$ and $S_2$ states of square cyclobutadiene obtained using state-optimized $\pi$-space CASSCF(4,4)-GIAO/6-311++G(2d,2p) wavefunctions (positive isovalue in blue).

$S_1$ electronic states of benzene and, less prominently, in the $S_2$ electronic state of square cyclobutadiene. In all three states the shielded regions near carbon-carbon bonds are mostly outside the rings; the shielding maxima observed within these regions are 25.33 ppm for $T_1$ $C_6H_6$, 22.69 ppm for $S_1$ $C_6H_6$ and 27.97 ppm for $S_2$ $C_4H_4$.

The isotropic shielding isosurfaces and contour plots for the $S_0$, $T_1$, $S_1$ and $S_2$ states of benzene and square cyclobutadiene in Figures 1–6 clearly show that, in terms of relative aromaticity, the eight electronic states studied in this paper are ordered from more aromatic to less aromatic (or more antiaromatic) as $S_2$ $C_6H_6$ > $S_0$ $C_6H_6$ > $T_1$ $C_4H_4$ > $S_1$ $C_4H_4$ > $S_2$ $C_4H_4$ > $S_0$ $C_4H_4$ > $T_1$ $C_6H_6$ > $S_1$ $C_6H_6$.

As can be seen in Figures 1–6, the shielded regions enveloping carbon-hydrogen bonds in antiaromatic electronic states ($S_0$ $C_4H_4$, $T_1$ $C_6H_6$ and $S_1$ $C_6H_6$) are, in general, larger and more intense than the corresponding regions in aromatic electronic states ($S_0$ $C_6H_6$, $S_2$ $C_6H_6$, $T_1$ $C_4H_4$ and $S_1$ $C_4H_4$). The noticeable overall deshielding of the molecular surroundings in $S_2$ $C_4H_4$ makes this electronic state
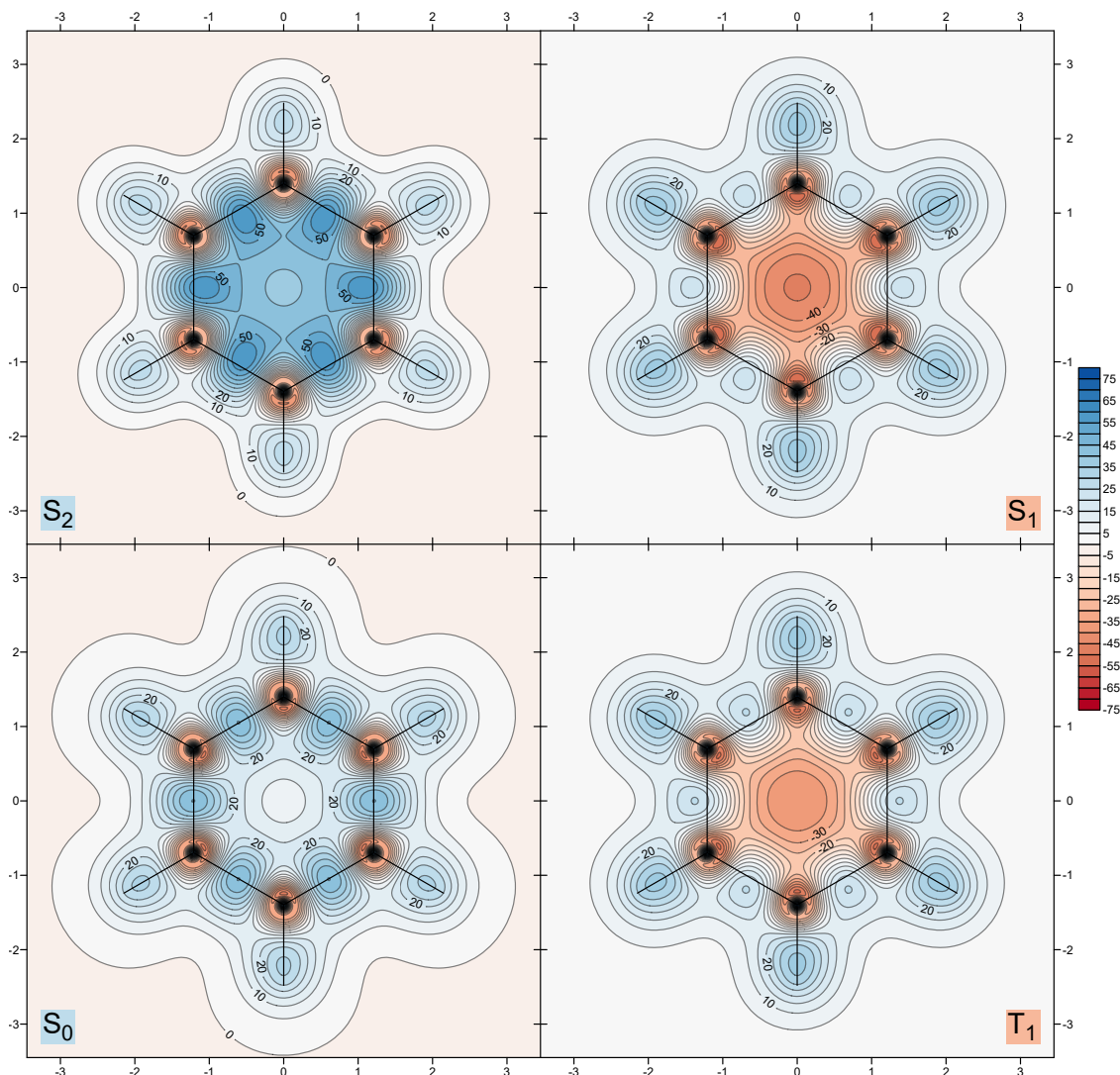
Figure 3: Isotropic shielding contour plots in the molecular (horizontal) plane for the $S_0$, $T_1$, $S_1$ and $S_2$ states of benzene (wavefunctions as for Figure 1, $\sigma_{iso}(\mathbf{r})$ in ppm, axes in Å).

an exception to the rule. Further confirmation of these observations is provided by the shielding maxima achieved along carbon-hydrogen bonds in antiaromatic electronic states (34.62 ppm in $S_0$ $C_4H_4$, 37.03 ppm in $T_1$ $C_6H_6$ and 37.18 ppm $S_1$ $C_6H_6$) which are higher than their counterparts in aromatic electronic states (31.36 ppm in $S_0$ $C_6H_6$, 27.29 ppm in $S_2$ $C_6H_6$, 31.52 ppm in $T_1$ $C_4H_4$ and 29.57 ppm in $S_1$ $C_4H_4$); the corresponding value for $S_2$ $C_4H_4$ is 27.30 ppm.

In all eight electronic states of benzene and square cyclobutadiene studied in this paper the carbon nuclei are surrounded by small, nearly spherical, shielded regions with radii under 0.07 Å inside each of which $\sigma_{iso}(\mathbf{r})$ rapidly falls from the respective $\sigma_{iso}(^{13}C)$ value to zero (see the dark circles around carbons in Figures 3–6). These small shielded regions are enclosed within larger ovoid deshielded regions, inside which the $\sigma_{iso}(\mathbf{r})$ values are negative. In an antiaromatic electronic state the ovoid deshielded regions
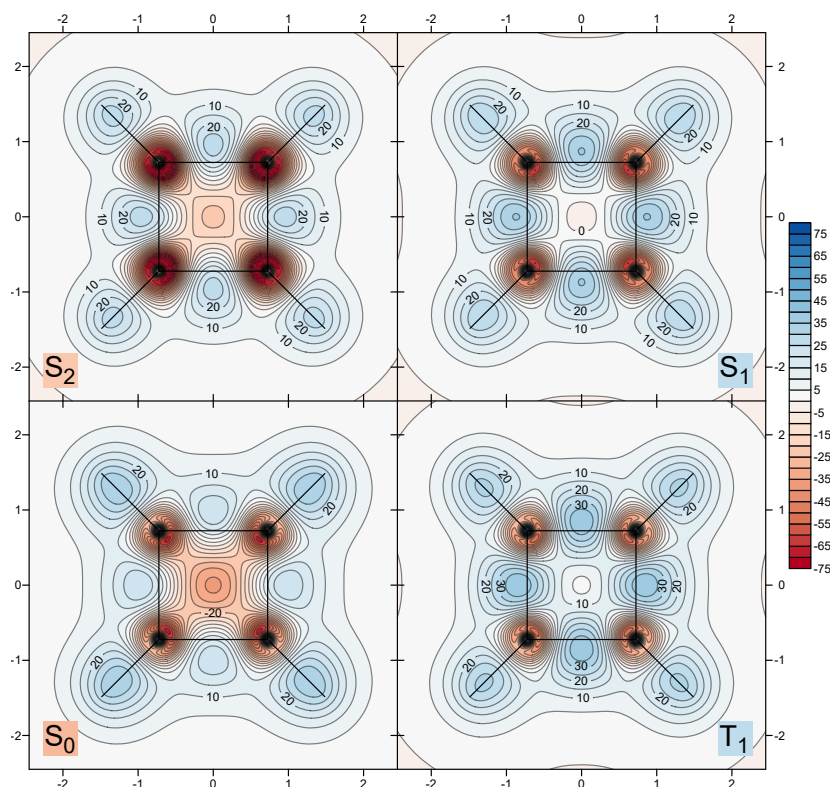
10

Figure 4: Isotropic shielding contour plots in the molecular (horizontal) plane for the $S_0$, $T_1$, $S_1$ and $S_2$ states of square cyclobutadiene (wavefunctions as for Figure 2, $\sigma_{\text{iso}}(\mathbf{r})$ in ppm, axes in Å).

around carbons merge with the larger deshielded region in the center of the molecule. Similar deshielded "halos" around sp$^2$ and sp hybridized carbons and other sp$^2$ hybridized second-row atoms have been observed previously, not only in conjugated rings,[19–21] but also in open-chain conjugated molecules such as ethene, ethyne and *s-trans*-1,3-butadiene.[22] This suggests that the deshielded "halos" are a sign of a specific type of $\pi$ electron behavior, characteristic of some sp$^2$ and sp hybridized second-row atoms and different from traditional ring currents. In general, the lowest $\sigma_{\text{iso}}(\mathbf{r})$ values within the deshielded "halos" in the electronic states of square cyclobutadiene ($-66.54$ ppm in $S_0$, $-52.94$ ppm in $T_1$, $-65.12$ ppm in $S_1$ and $-102.42$ ppm in $S_2$) are lower than their counterparts in benzene ($-46.44$ ppm in $S_0$, $-51.07$ ppm in $T_1$, $-54.87$ ppm in $S_1$ and $-40.39$ ppm in $S_2$); in each molecule the "halos" are more deshielded in antiaromatic electronic states.

In principle, isotropic shielding isosurfaces and contour plots can be used to analyze chemical bonding and, for cyclic conjugated systems, aromaticity and antiaromacity, in any electronic state that can be described reliably by a wavefunction for which one can compute off-nucleus magnetic shielding tensors. At present, the only way to target electronic states other than the ground state is to utilize the MCSCF-GIAO code in Dalton[27] which is capable of performing state-optimized CASSCF-GIAO calculations. This would create certain computational difficulties if an attempt were made to analyze the
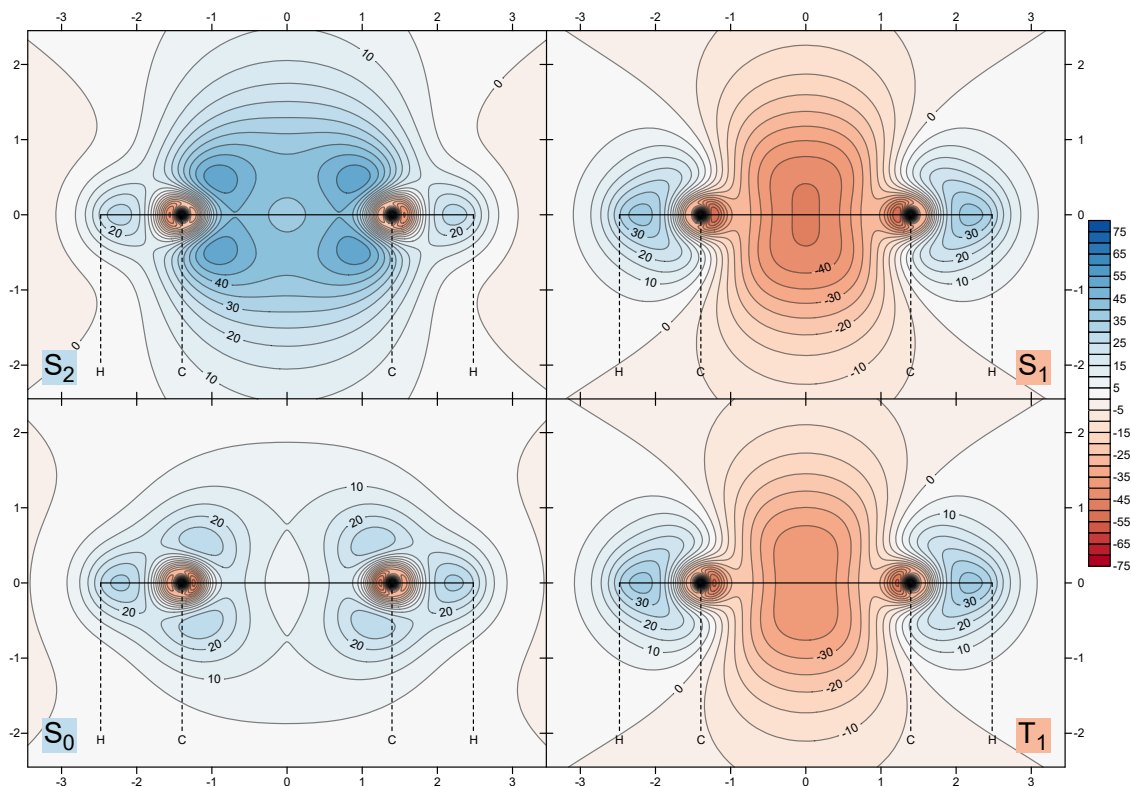
11

Figure 5: Isotropic shielding contour plots in the vertical plane passing through two carbons and two hydrogens for the $S_0$, $T_1$, $S_1$ and $S_2$ states of benzene (wavefunctions as for Figure 1, $\sigma_{\mathrm{iso}}(\mathbf{r})$ in ppm, axes in Å).

aromaticities of higher electronic states of benzene and square cyclobutadiene. Let us take benzene as an example. As it was already mentioned, the order of the $S_3$ and $S_4$ electronic states is reversed in $\pi$-space CASSCF(6,6) calculations. Getting these states in the correct order requires inclusion of dynamic correlation between the electrons in $\sigma$ and $\pi$ orbitals, which would also help with obtaining more accurate vertical excitation energies for $S_2$ and higher electronic states. Additionally, each of the $S_3$ ($1\,^1E_{1u}$) and $S_4$ ($1\,^1E_{2g}$) electronic states is doubly-degenerate, and so is $T_2$ ($1\,^3E_{1u}$). The standard way of dealing with degenerate electronic states is to perform state-averaged CASSCF calculations. So, making progress with higher electronic states of benzene would require, as a minimum, a SA-CASSCF code with GIAOs; for more accurate results, one would also need a code capable of calculating magnetic shielding tensors with GIAOs using CASPT2 or another multireference perturbation theory approach.

## 4    CONCLUSIONS

The analysis of the spatial variations in isotropic shielding, $\sigma_{\mathrm{iso}}(\mathbf{r})$, for the ground, lowest triplet and first and second singlet excited electronic states of benzene and square cyclobutadiene demonstrates that
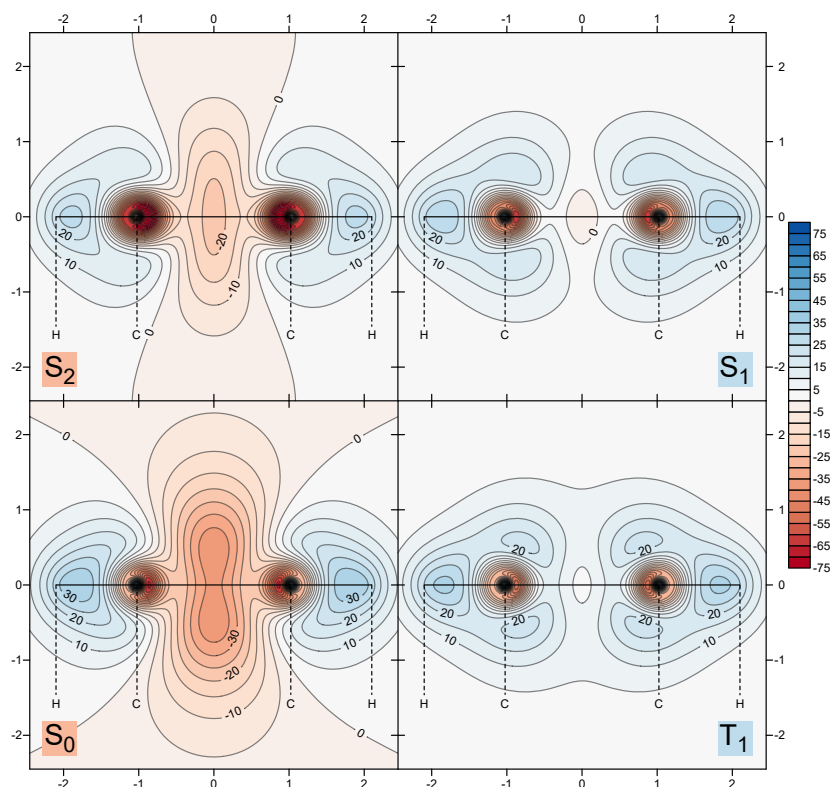
Figure 6: Isotropic shielding contour plots in the vertical plane passing through two carbons and two hydrogens for the $S_0$, $T_1$, $S_1$ and $S_2$ states of square cyclobutadiene (wavefunctions as for Figure 2, $\sigma_{\mathrm{iso}}(\mathbf{r})$ in ppm, axes in Å).

the key features of one of the two profoundly different isotropic shielding distributions in the electronic ground states of these molecules, reported initially in Ref. 19 and confirmed in the current work, are reproduced, with a substantial degree of similarity, in each of the other low-lying electronic states that were investigated.

The doughnut-shaped region of increased shielding enclosing the carbon ring in the electronic ground state of benzene, which is indicative of strong bonding interactions and aromatic stability, is also observed in the lowest triplet and first singlet electronic excited states of square cyclobutadiene. In the second singlet excited electronic state of benzene which, according to the results of this work, is even more aromatic than the ground state, the whole interior of the carbon ring is so intensely shielded that the $\sigma_{\mathrm{iso}}(\mathbf{r}) = 16$ ppm isosurface we usually examine becomes nearly spherical in shape, with small indentations around the carbon atoms.

The main cause for antiaromatic destabilization in the ground electronic state of square cyclobuta-diene, a sizable markedly deshielded region in the center of the molecule which disrupts the linkages between the shielded regions corresponding to individual carbon-carbon bonds and thus weakens these bonds, is also present, even more prominently, in the lowest triplet and first singlet electronic excited

states of benzene. This antiaromatic feature is still obvious but less pronounced in the isotropic shielding distribution for the second singlet excited electronic state of square cyclobutadiene.

These observations indicate that the isotropic shielding distributions in the electronic ground states of benzene and square cyclobutadiene represent general aromaticity and antiaromaticity "fingerprints" that can be used to identify the aromatic character of an electronic state of a cyclic conjugated system.

Benzene starts as aromatic in its electronic ground state, becomes antiaromatic in the first singlet excited state, then reverts to aromatic in the second singlet excited state. Square cyclobutadiene alternates between antiaromatic in the electronic ground state, aromatic in the first singlet excited state, and antiaromatic in the second singlet excited state. These sequences suggest an aromaticity rule for singlet excited electronic states, according to which Hückel-aromatic rings with $4n + 2$ $\pi$ electrons become antiaromatic in the first singlet excited state and switch back to aromatic in the second singlet excited state, whereas Hückel-antiaromatic rings with $4n$ $\pi$ electrons become aromatic in the first singlet excited state and revert to antiaromatic in the second singlet excited state.

The most important advantage of the analysis of the spatial variations in isotropic shielding over single value aromaticity indices is that, in addition to providing information about relative aromaticity and antiaromaticity, the isotropic shielding isosurfaces and contour plots show very clearly the effects of aromaticity and antiaromaticity on chemical bonding which, arguably, can be viewed as the most succinct visual definitions of these phenomena currently available.

# Associated Content

**Supporting Information**

GAUSSIAN cube files containing all $\sigma_{\mathrm{iso}}(\mathbf{r})$ values for the $S_0$, $T_1$, $S_1$ and $S_2$ states of benzene and square cyclobutadiene obtained in the current paper. This material is available free of charge via the Internet at http://pubs.acs.org/.

# AUTHOR INFORMATION

**Corresponding Author**

*E-mail: peter.karadakov@york.ac.uk

**Notes**

The authors declare no competing financial interest.

## REFERENCES

(1) Rosenberg, M.; Dahlstrand, C.; Kilså, K.; Ottosson, H. *Chem. Rev.* **2014**, *114*, 5379–5425.

(2) Sung, Y. M.; Yoon, M.-C.; Lim, J. M.; Rath, H.; Naoda, K.; Osuka, A.; Kim, D. *Nature Chem.* **2015**, *7*, 418–422.

(3) Sung, Y. M.; Oh, J.; Kim, W.; Mori, H.; Osuka, A.; Kim, D. *J. Am. Chem. Soc.* **2015**, *137*, 11856–11859.

(4) Baird, N. C. *J. Am. Chem. Soc.* **1972**, *94*, 4941–4948.

(5) Karadakov, P. B. *J. Phys. Chem. A* **2008**, *112*, 7303–7309.

(6) Karadakov, P. B. *J. Phys. Chem. A* **2008**, *112*, 12707–12713.

(7) Ottosson, H.; Borbas, K. E. *Nature Chem.* **2015**, *7*, 373–375.

(8) Schleyer, P. v. R.; Maerker, C.; Dransfeld, A.; Jiao, H.; Hommes, N. J. R. v. E. *J. Am. Chem. Soc.* **1996**, *118*, 6317–6318.

(9) Schleyer, P. v. R.; Jiao, H.; Hommes, N. J. R. v. E.; Malkin, V. G.; Malkina, O. L. *J. Am. Chem. Soc.* **1997**, *119*, 12669–12670.

(10) Schleyer, P. v. R.; Manoharan, M.; Wang, Z. X.; Kiran, B.; Jiao, H.; Puchta, R.; Hommes, N. J. R. v. E. *Org. Lett.* **2001**, *3*, 2465–2468.

(11) Cernusak, I.; Fowler, P. W.; Steiner, E. *Mol. Phys.* **2000**, *98*, 945–953.

(12) Steiner, E.; Fowler, P. W.; Jenneskens, L. W. *Angew. Chem. Int. Ed.* **2001**, *40*, 362–366.

(13) Fallah-Bagher-Shaidaei, H.; Wannere, C. S.; Corminboeuf, C.; Puchta, R.; Schleyer, P. v. R. *Org. Lett.* **2006**, *8*, 863–866.

(14) Feixas, F.; Vandenbussche, J.;Bultinck, P; Matitoc, E.; Solà, M. *Phys. Chem. Chem. Phys.* **2011**, *13*, 20690–20703.

(15) Klod, S.; Kleinpeter, E. *J. Chem. Soc., Perkin Trans. 2* **2001**, 1893–1898.

(16) Kleinpeter, E.; Klod, S.; Koch, A. *J. Mol. Struct. THEOCHEM* **2007**, *811*, 45–60.

(17) Kleinpeter, E.; Koch, A. *Phys. Chem. Chem. Phys.* **2012**, *14*, 8742–8746.

(18) Kleinpeter, E.; Koch, A. *J. Phys. Chem. A* **2012**, *116*, 5674–5680.

(19) Karadakov, P. B.; Horner, K. E. *J. Phys. Chem. A* **2013**, *117*, 518–523.

(20) Horner, K. E.; Karadakov, P. B. *J. Org. Chem.* **2013**, *78*, 8037–8043.

(21) Horner, K. E.; Karadakov, P. B. *J. Org. Chem.* **2015**, *80*, 7150–7157.

(22) Karadakov, P. B.; Horner, K. E. *J. Chem. Theory Comput.* **2016**, *12*, 558–563.

(23) Fias, S.; Fowler, P. W.; Delgado, J. L.; Hahn, U.; Bultinck, P. *Chem. Eur. J.* **2008**, *14*, 3093–3099.

(24) Van Damme, S.; Acke, G.; Havenith, R. W. A.; Bultinck, P. *Phys. Chem. Chem. Phys.* **2016**, *18*, 11746–11755.

(25) Ruud, K.; Helgaker, T.; Kobayashi, R.; Jørgensen, P.; Bak, K. L.; Jensen, H. J. A. *J. Chem. Phys.* **1994**, *100*, 8178–8185.

(26) Ruud, K.; Helgaker, T.; Bak, K. L.; Jørgensen, P.; Olsen, J. *Chem. Phys.* **1995**, *195*, 157–169.

(27) Aidas, K.; Angeli, C.; Bak, K. L.; Bakken, V.; Bast, R.; Boman, L.; Christiansen, O.; Cimiraglia, R.; Coriani, S.; Dahle, P.; Dalskov, E. K.; Ekström, U.; Enevoldsen, T.; Eriksen, J. J.; Ettenhuber, P.; Fernández, B.; Ferrighi, L.; Fliegl, H.; Frediani, L.; Hald, K.; Halkier, A.; Hättig, C.; Heiberg, H.; Helgaker, T.; Hennum, A. C.; Hettema, H.; Hjertenæs, R.; Høst, S.; Høyvik, I.-M.; Iozzi, M. F.; Jansík, B.; Jensen, H. J. Aa.; Jonsson, D.; Jørgensen, P.; Kauczor, J.; Kirpekar, S.; Kjærgaard, T.; Klopper, W.; Knecht, S.; Kobayashi, R.; Koch, H.; Kongsted, J.; Krapp, A.; Kristensen, K.; Ligabue, A.; Lutnæs, O. B.; Melo, J. I.; Mikkelsen, K. V.; Myhre, R. H.; Neiss, C.; Nielsen, C. B.; Norman, P.; Olsen, J.; Olsen, J. M. H.; Osted, A.; Packer, M. J.; Pawlowski, F.; Pedersen, T. B.; Provasi, P. F.; Reine, S.; Rinkevicius, Z.; Ruden, T. A.; Ruud, K.; Rybkin, V. V.; Sałek, P.; Samson., C. C. M.; Sánchez de Merás, A.; Saue, T.; Sauer, S. P. A.; Schimmelpfennig, B.; Sneskov, K.; Steindal, A. H.; Sylvester-Hvid, K. O.; Taylor, P. R.; Teale, A. M.; Tellgren, E. I.; Tew, D. P.; Thorvaldsen, A. J.; Thøgersen, L.; Vahtras, O.; Watson, M. A.; Wilson, D. J. D.; Ziolkowski, M.; Ågren, H. *WIREs Comput. Mol. Sci.* **2014**, *4*, 269–284; *Dalton, a Molecular Electronic Structure Program, Release Dalton2016.0*, **2015**, see http://daltonprogram.org.

(28) Cabana, A.; Bachand, J.; Giguère, J. *Can. J. Phys.* **1974**, *52*, 1949–1955.

(29) Eckert-Maksić, M.; Vazdar, M.; Barbatti, M.; Lischka, H.; Maksić, Z. B. *J. Chem. Phys.* **2006**, *125*, 064310, 1–9.

(30) Gogonea, V.; Schleyer, P. v. R.; Schreiner, P. R. *Angew. Chem. Int. Ed.*, *37*, 1945–1948.

(31) Fowler, P. W.; Steiner, E.; Jenneskens, L. W. *Chem. Phys. Lett.* **2003**, *371*, 719–723.

(32) Rinkevicius, Z.; Vaara, J.; Telyatnyk, L.; Vahtras, O. *J. Chem. Phys.* **2003**, *118*, 2550–2561.

(33) Vaara, J. *Phys. Chem. Chem. Phys.* **2007**, *9*, 5399–5418.

(34) See http://www.gaussian.com/g_tech/g_ur/u_cubegen.htm.

(35) Doering, J. P. *J. Chem. Phys.* **1969**, *51*, 2866-2870.

(36) Lassettre, E. N.; Skerbele, A.; Dillon, M. A.; Ross, K. J. *J. Chem. Phys.* **1968**, *48*, 5066–5096.

(37) da Silva, E. C.; Gerratt, J.; Cooper, D. L.; Raimondi, M. *J. Chem. Phys.* **1994**, *101*, 3866–3887.

(38) Nakamura, K.; Osamura, Y.; Iwata, S. *Chem. Phys.* **1989**, *136*, 67–77.

(39) Roos, B. O.; Andersson, K.; Fülscher, M. P. *Chem. Phys. Lett* **1992**, *192*, 5–13.